# Electronic Supplemental Information

# Single-step solution plasma synthesis of bifunctional $CoSn(OH)_6$-carbon composite electrocatalysts for oxygen evolution and oxygen reduction reactions

Sangwoo Chae[1], Akihito Shio[2], Taketo Imamura[2], Kouki Yamamoto[2], Yuna Fujiwara[2], Gasidit Panomsuwan[3], Takahiro Ishizaki[4*]

[1]SIT Research Laboratories, Shibaura Institute of Technology, Tokyo 135-8548, Japan

(Present address: Institutes of Innovation for Future Society Designated, Nagoya University, Japan)

[2]Materials Science and Engineering, Graduate School of Engineering and Science, Shibaura Institute of Technology, Toyosu, Koto-Ku, Tokyo, 135-8548, Japan

[3]Department of Materials Engineering, Faculty of Engineering, Kasetsart University, Bangkok 10900, Thailand

[4]College of Engineering, Shibaura Institute of Technology, Tokyo 135-8548, Japan

*Corresponding author: ishizaki@shibaura-it.ac.jp

## XRD patterns of the composite materials synthesized by coprecipitation method

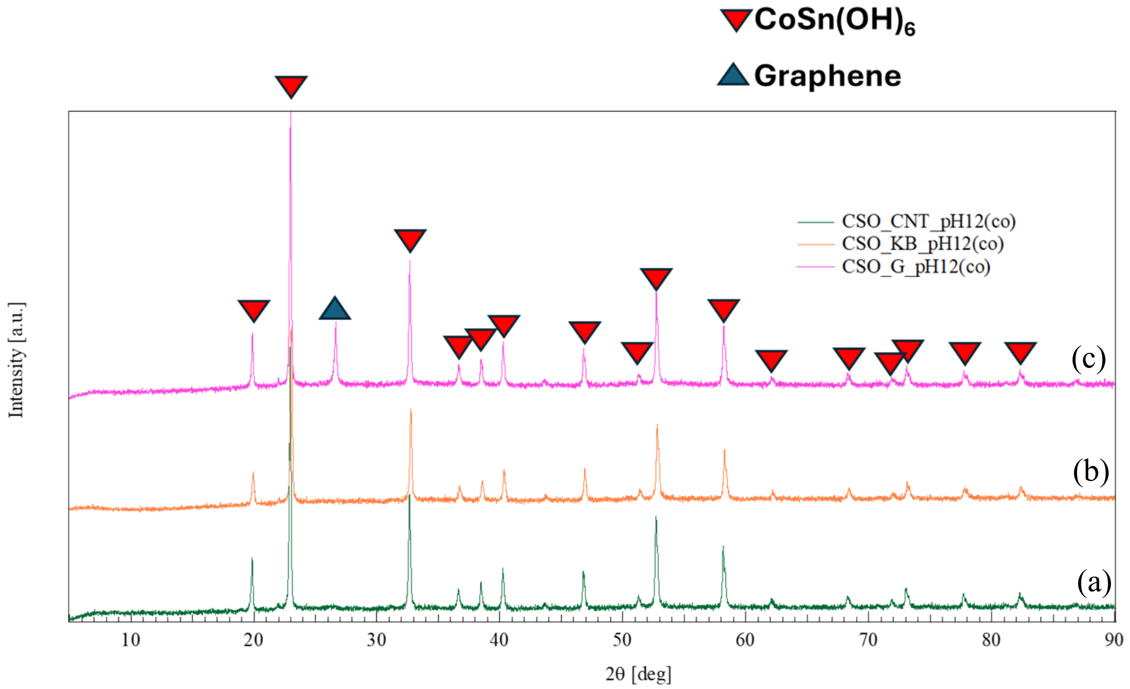

Figure S1. XRD patterns of (a) CSO_CNT_ pH 12 (co), (b) CSO_G_ pH 12 (co), and (c) CSO_KB_ pH 12 (co).

## FE-SEM images

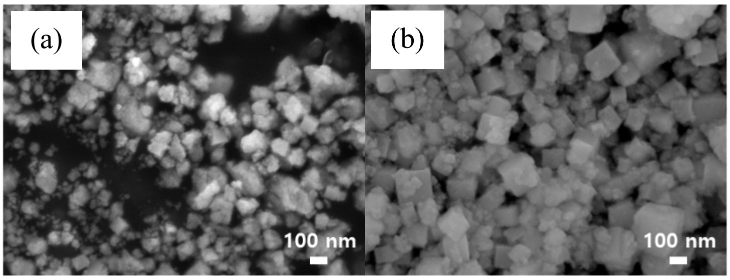

Figure S2. FE-SEM images of (a) CSO_ pH10，(b) CSO_ pH12.

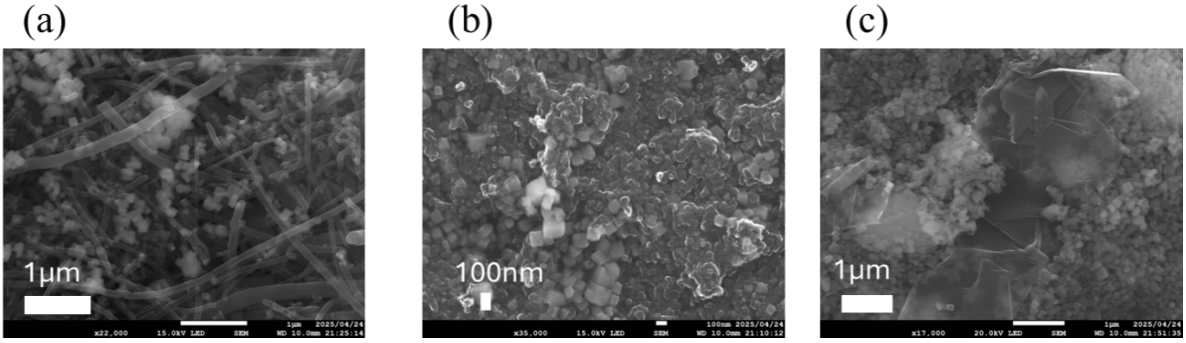

Figure S3. FE-SEM images of (a) CSO_CNT_ pH 12 (co), (b) CSO_G_ pH 12 (co), and (c) CSO_KB_ pH 12 (co).

## TEM images

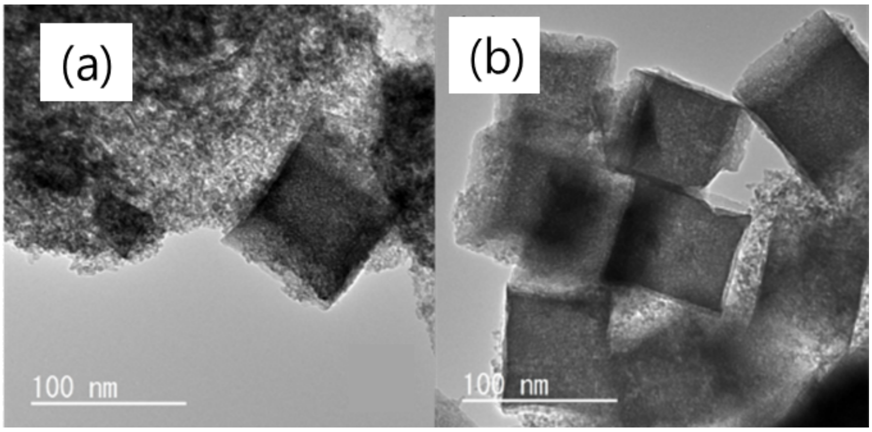

Figure S4. TEM images of (a) CSO_pH10，(b) CSO_ pH12

**STEM and EDS measurements**

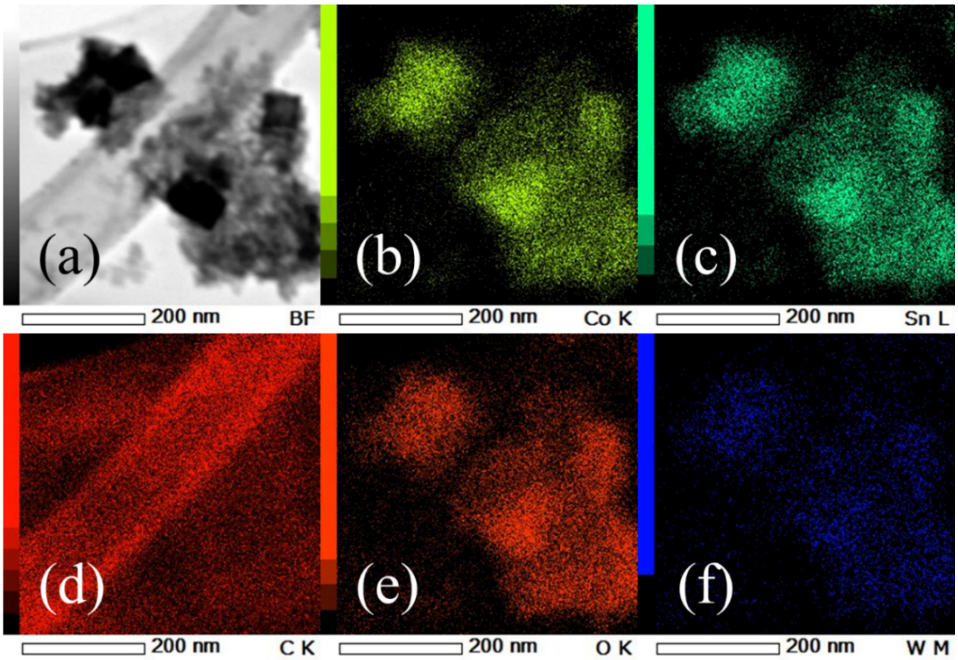

Figure S5 STEM image of the CSO_CNT_pH10, (a) EDS mapping images of CSO_CNT_pH10 in (b-f) confirming the presence of Co, Sn, C, O and W.

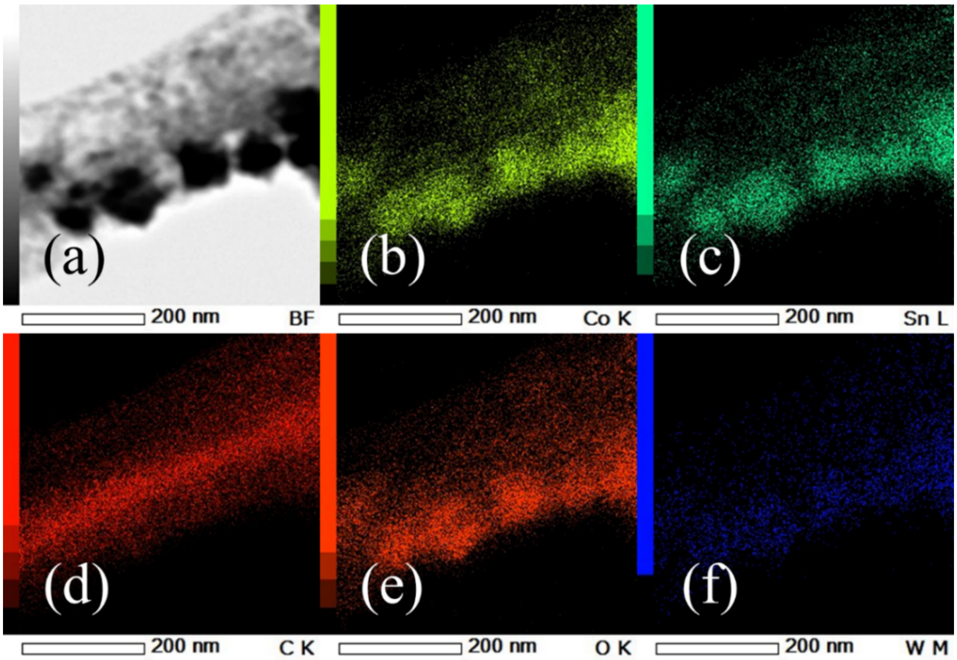

Figure S6 image of the CSO_G_pH10, (a) EDS mapping images of CSO_G_pH10 in (b-f) confirming the presence of Co, Sn, C, O and W.

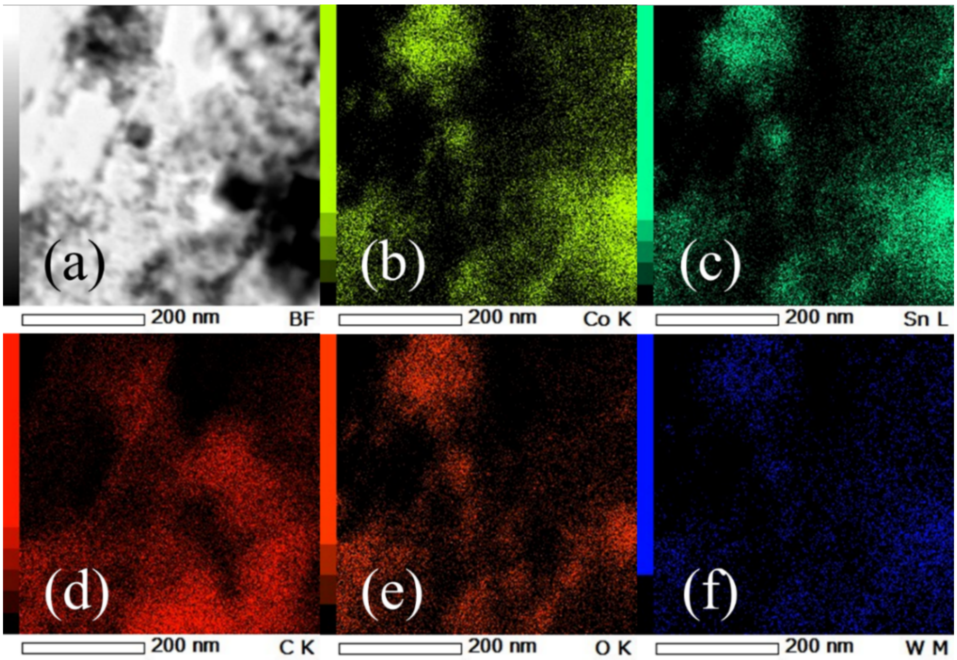

Figure S7 image of the CSO_KB_pH10, (a) EDS mapping images of CSO_KB_pH10 in (b-f) confirming the presence of Co, Sn, C, O and W.

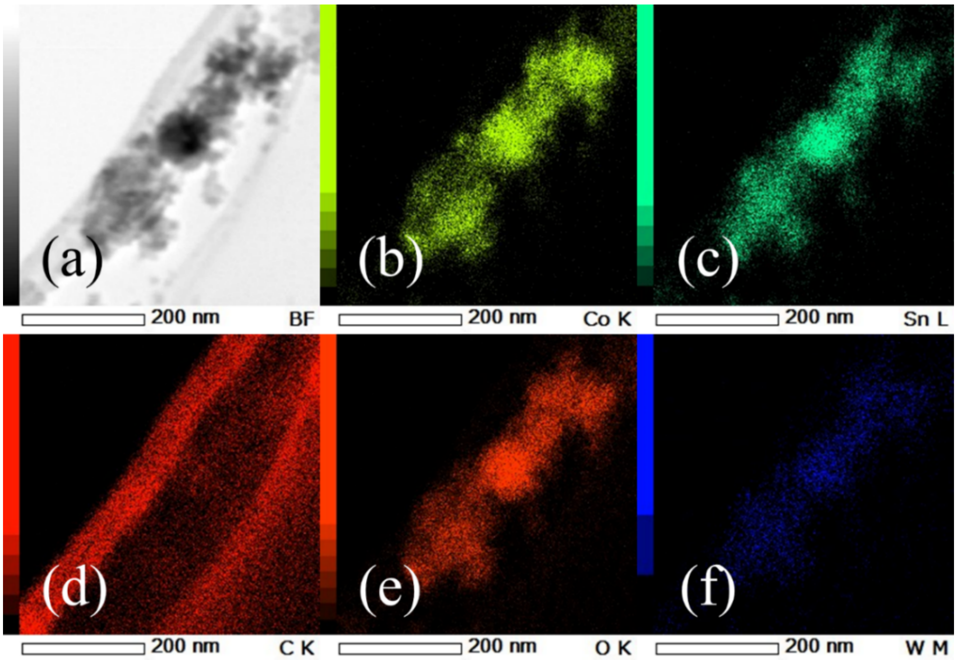

Figure S8 STEM image of the CSO_CNT_pH12, (a) EDS mapping images of CSO_CNT_pH12 in (b-f) confirming the presence of Co, Sn, C, O and W.

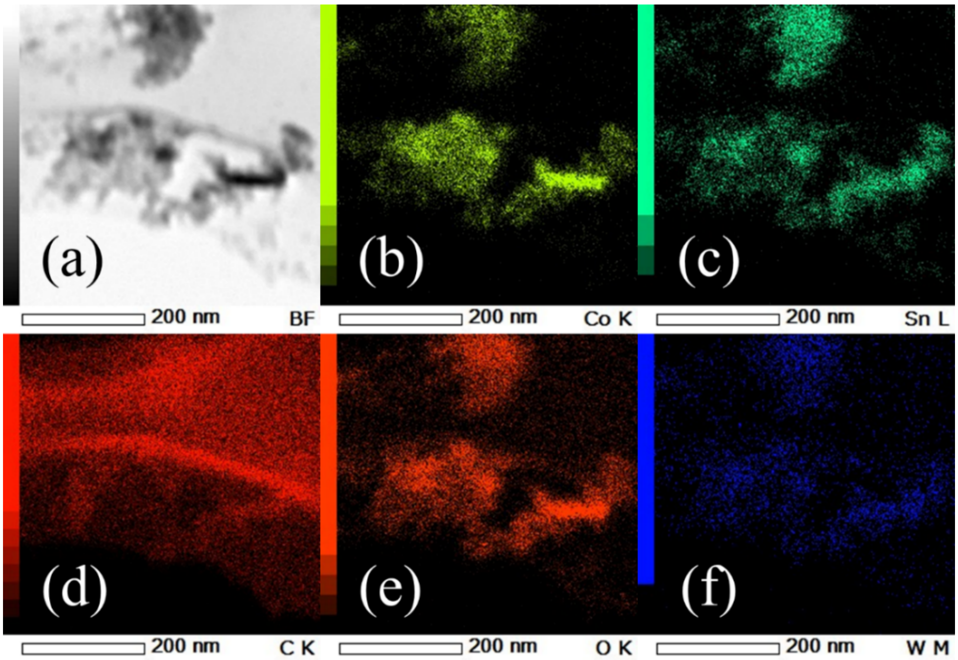

Figure S9 STEM image of the CSO_G_12, (a) EDS mapping images of CSO_G_12 in (b-f) confirming the presence of Co, Sn, C, O and W.

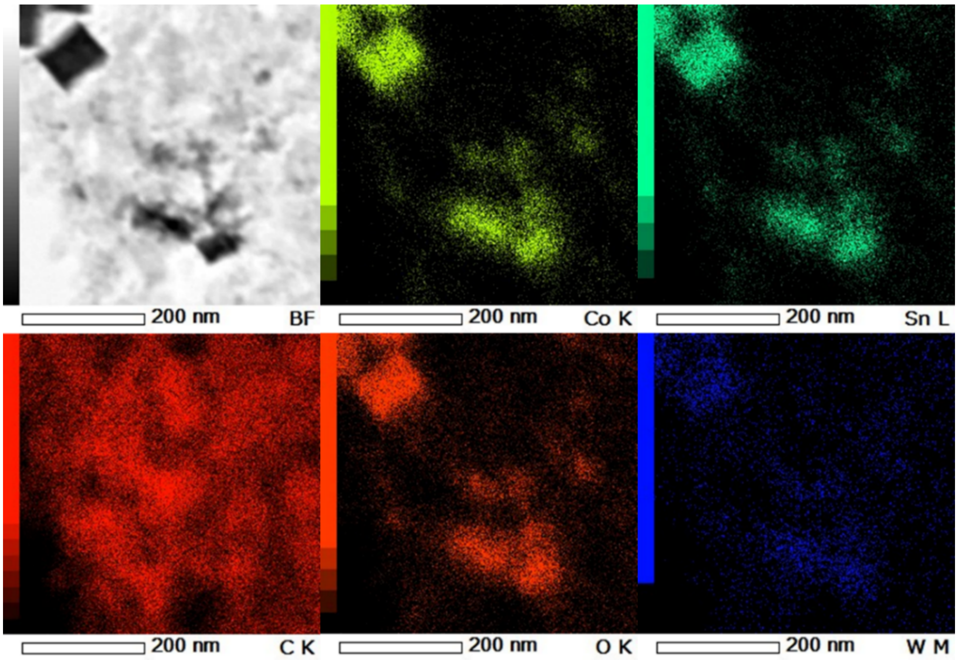

Figure S10 STEM image of the CSO_KB_12, (a) EDS mapping images of CSO_KB_12 in (b-f) confirming the presence of Co, Sn, C, O and W.

## XPS measurements

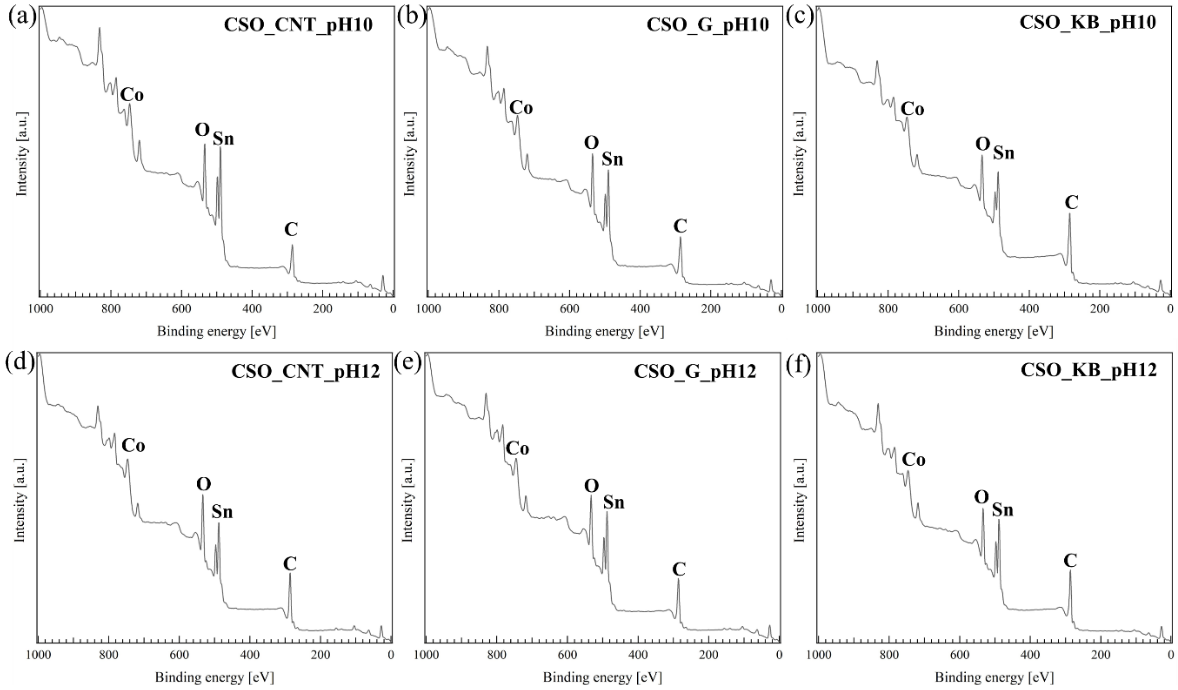

Figure S11. XPS wide spectra of the samples synthesized by SP: (a) CSO_CNT_pH10, (b) CSO_G_pH10, (c) CSO_KB_pH10, (d) CSO_CNT_pH12, (e) CSO_G_pH12, and (f) CSO_CNT_pH12.

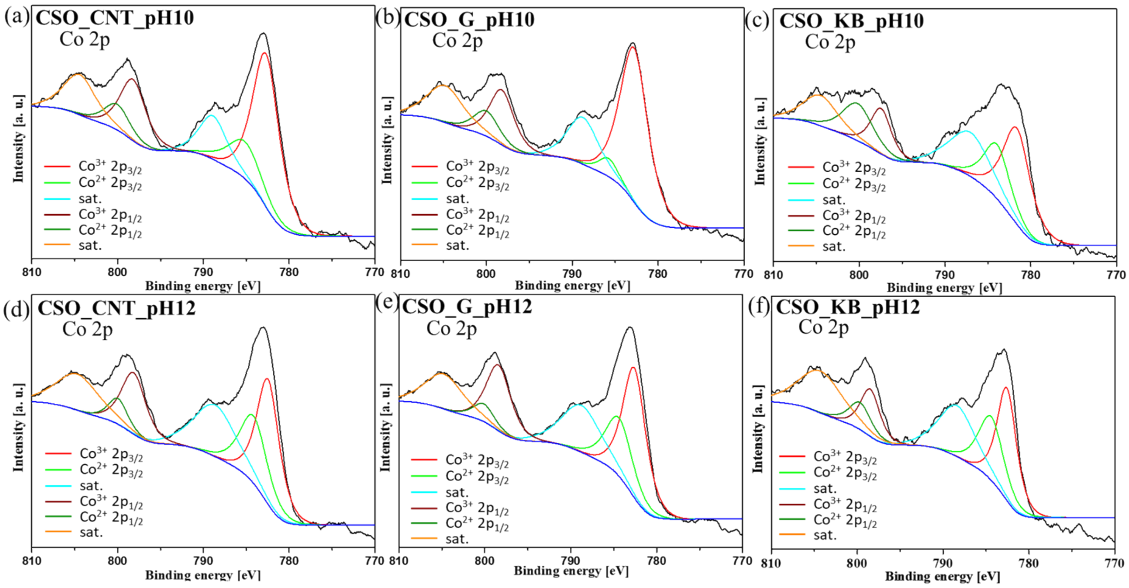

Figure S12. High-resolution XPS Co 2*p* spectra of the samples synthesized by SP: (a) CSO_CNT_pH10, (b) CSO_G_pH10, (c) CSO_KB_pH10, (d) CSO_CNT_pH12, (e) CSO_G_pH12, and (f) CSO_CNT_pH12.

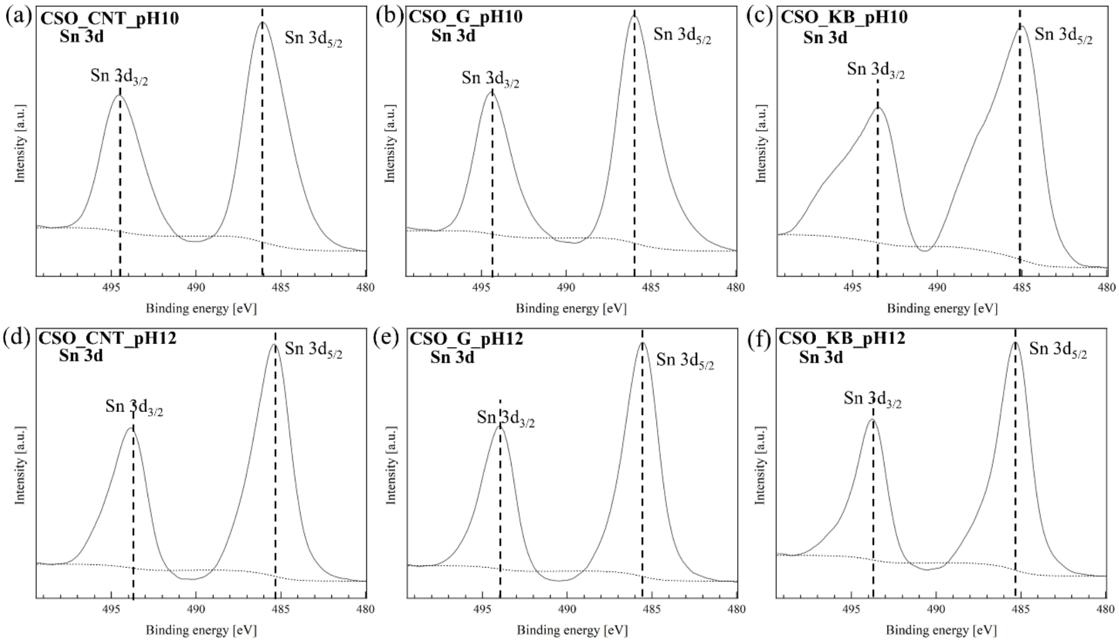

Figure S13. High-resolution XPS Sn 3*d* spectra of the samples synthesized by SP: (a) CSO_CNT_pH10, (b) CSO_G_pH10, (c) CSO_KB_pH10, (d) CSO_CNT_pH12, (e) CSO_G_pH12, and (f) CSO_CNT_pH12.

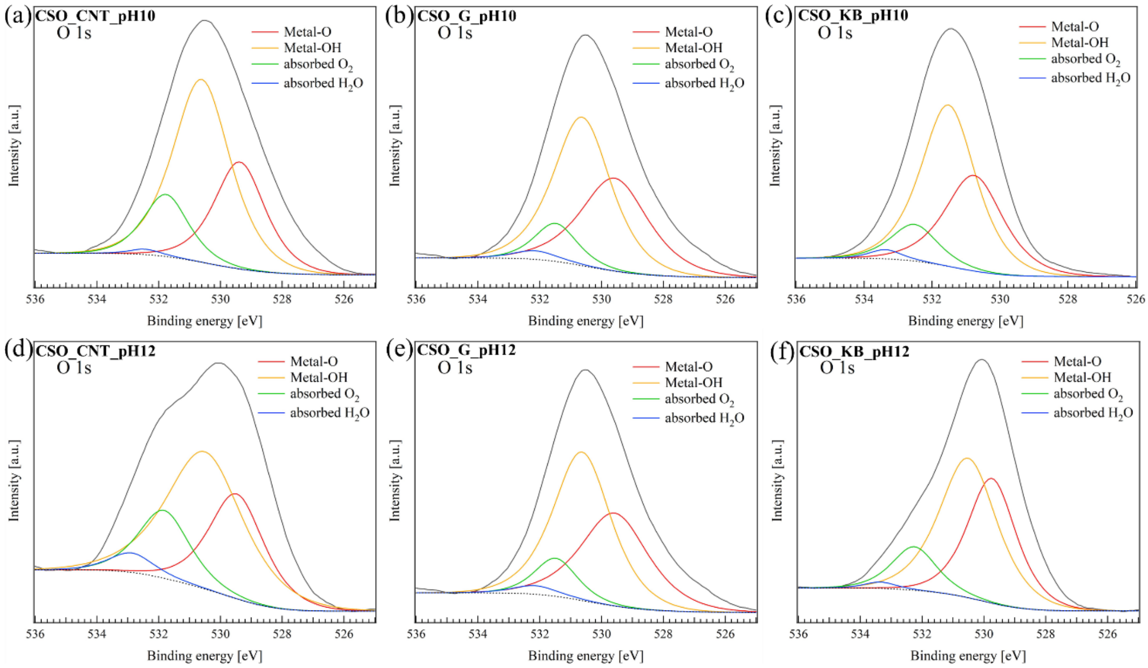

Figure S14. High-resolution XPS O 1*S* spectra of the samples synthesized by SP: (a) CSO_CNT_pH10, (b) CSO_G_pH10, (c) CSO_KB_pH10, (d) CSO_CNT_pH12, (e) CSO_G_pH12, and (f) CSO_CNT_pH12.

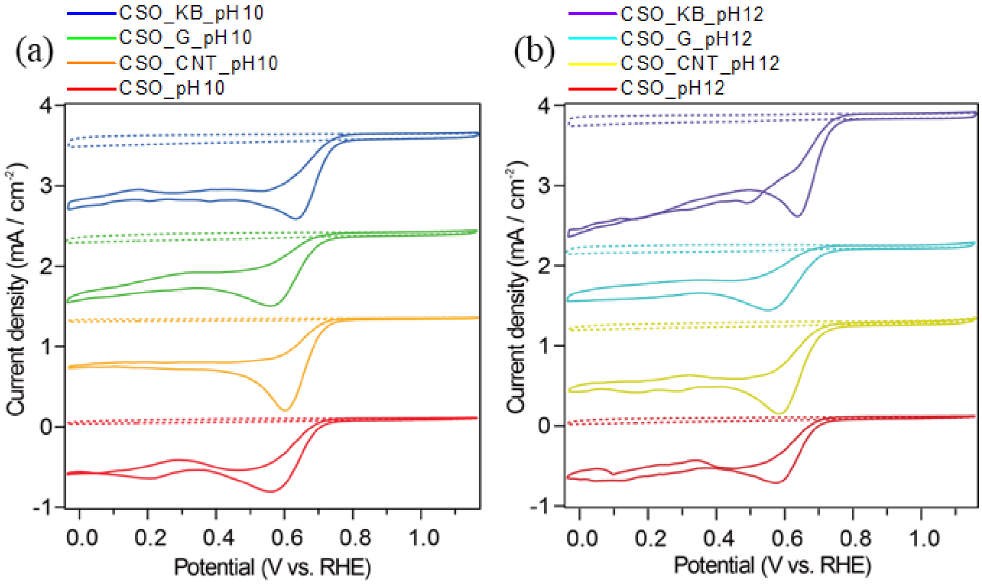

Figure S15. Electrochemical evaluations of the samples synthesized at (a) pH = 10 and (b) pH = 12. CV curves in $N_2$ and $O_2$-saturated 1 M KOH solutions at a scan rate of 50 mV/s ($N_2$: dashed line, $O_2$: solid line).

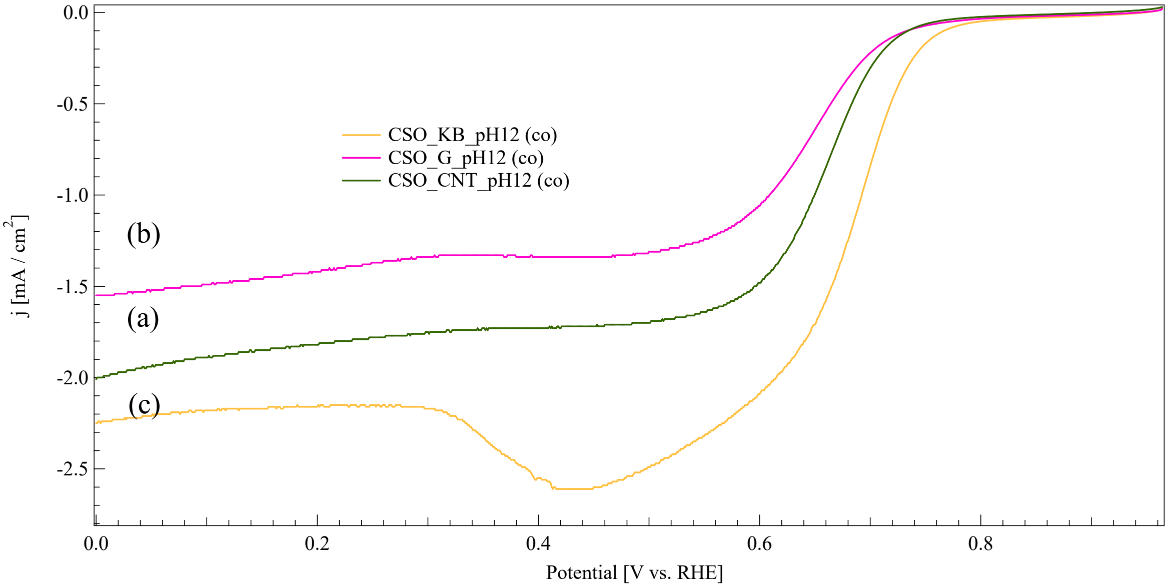

Figure S16. LSV curves using an RRDE electrode in an $O_2$-saturated 1 M KOH solution at a scan rate of 10 mV/s. The rotation speed was 1600 rpm; (a) CSO_CNT_ pH 12 (co), (b) CSO_G_ pH 12 (co), and (c) CSO_KB_ pH 12 (co).

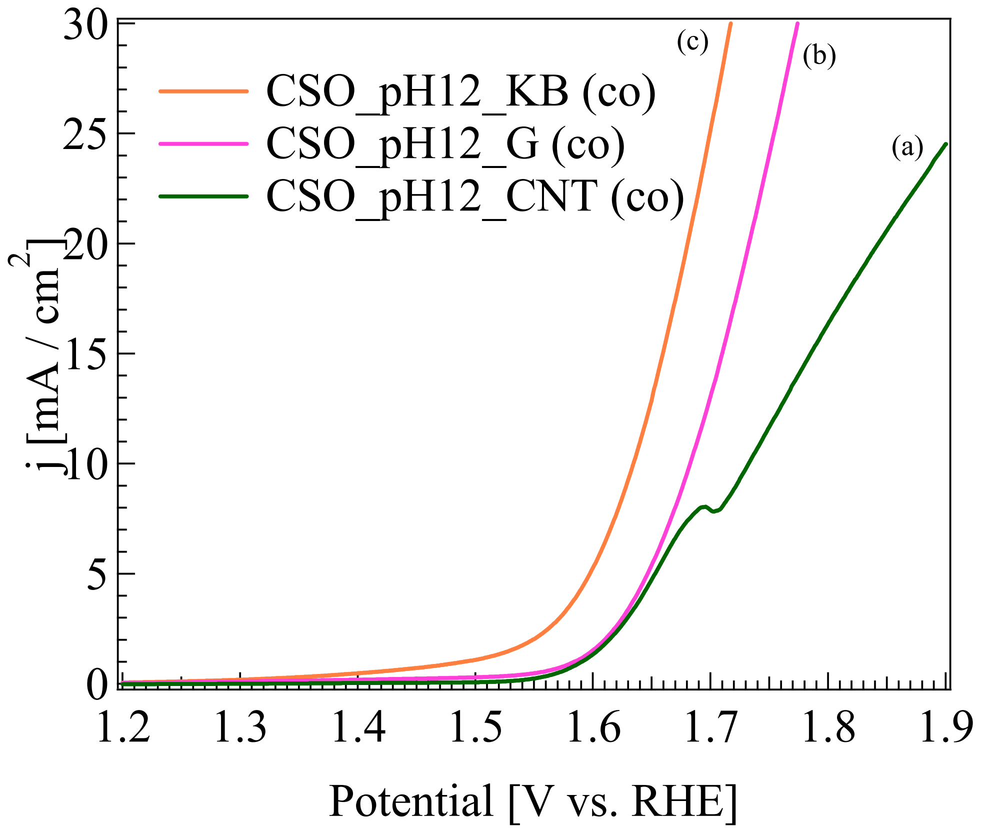

Figure S17. LSV curves of the composite samples synthesized by coprecipitation method at pH = 12: (a) CSO_CNT_ pH 12 (co), (b) CSO_G_ pH 12 (co), and (c) CSO_KB_ pH 12 (co).

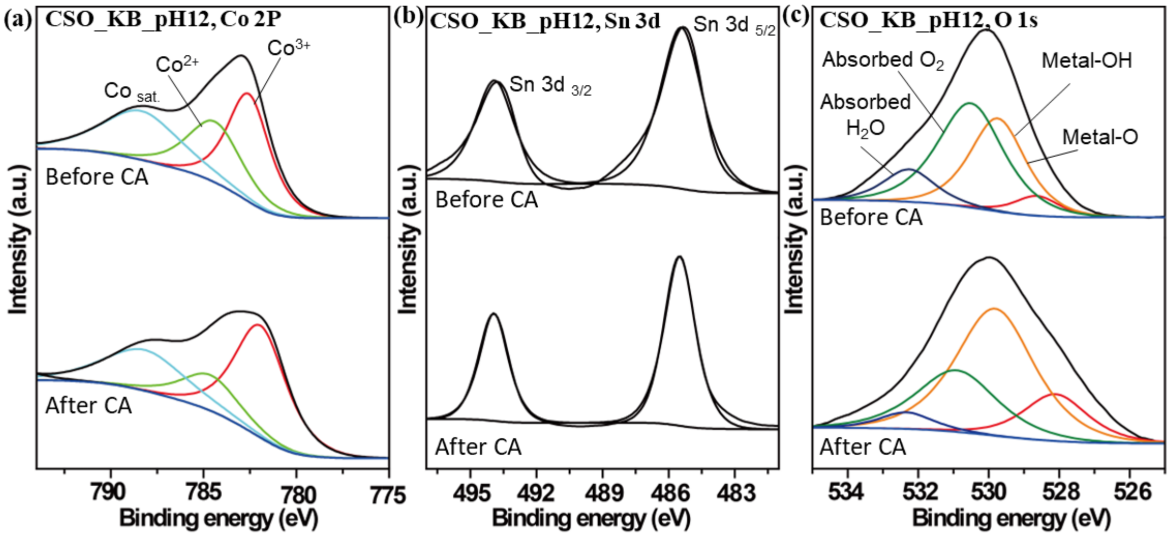

Figure S18. High-resolution XPS of (a) Co 2*p*, (b) Sn 3*d*, and (c) O 1*s* spectra for CSO_KB_pH12 before and after the CA measurement.

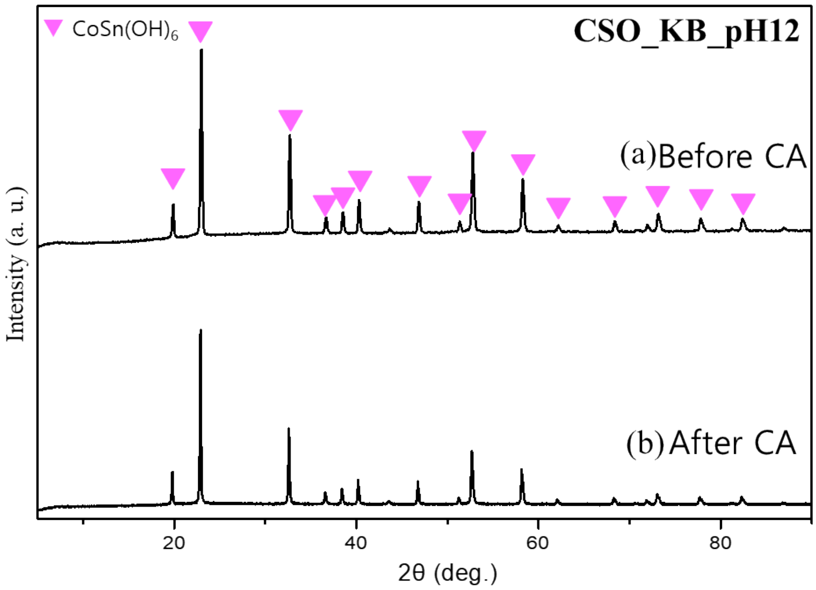

Figure S19. XRD patterns of CSO_KB_pH12 (a) before and (b) after the CA measurement.

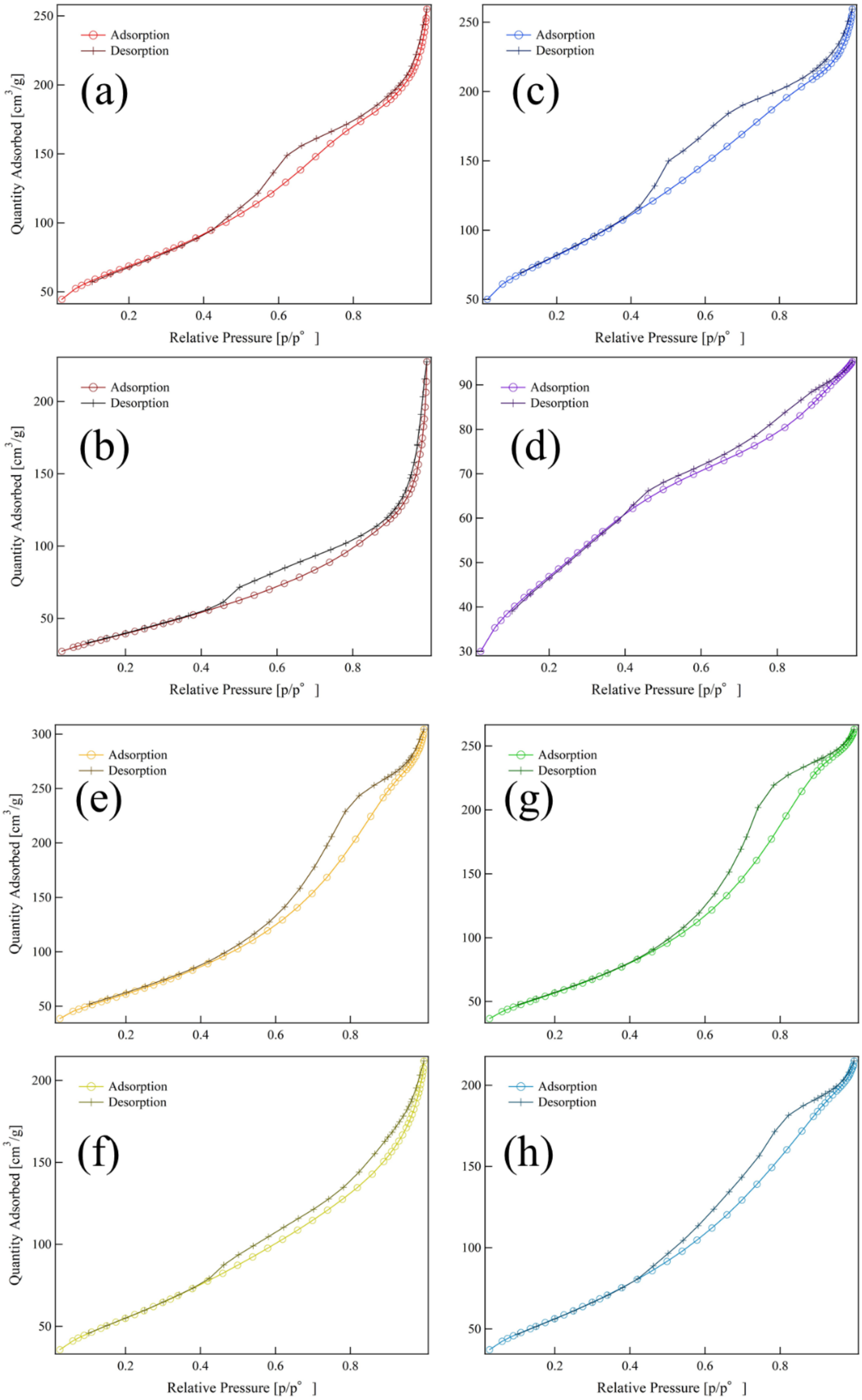

Figure S20. $N_2$ adsorption isotherm curves of (a) CSO_pH10，(b) CSO_pH12，(c) CSO_KB_pH10，(d) CSO_KB_pH12，(e) CSO_ CNT_pH10，(f) CSO_CNT_ pH12，(g) CSO_G_pH10，and (h) CSO_G_pH12.

## Solution plasma conditions

Table S1 SPP Conditions (CSO)

| Sample | CSO_pH10 | CSO_CNT_pH10 | CSO_G_pH10 | CSO_KB_pH10 | CSO_pH12 | CSO_CNT_pH12 | CSO_G_pH12 | CSO_KB_pH12 |
|---|---|---|---|---|---|---|---|---|
| Applied voltage | 1.2 kV | | | | | | | |
| frequency | 50 kHz | | | | | | | |
| pulse width | 0.8 µsec | | | | | | | |
| Distance between electrodes | 0.5 mm | | | | | | | |
| Discharge time | 20 min | | | | | | | |
| Solution pH | 10 | | | | 12 | | | |
| Carbon mixture amount | - | CNT<br>25 mg | G<br>25 mg | KB<br>25 mg | - | CNT<br>25 mg | G<br>25 mg | KB<br>25 mg |
| Electrode | W (Diameter: 1.0 mm) | | | | | | | |

Table S2 Quantitative analysis results of each sample (at.%)

| Sample | Co | Sn | O | W |
|---|---|---|---|---|
| CSO_CNT_pH10 | 26.25 | 27.29 | 46.46 | - |
| CSO_G_pH10 | 31.80 | 30.90 | 37.23 | 0.07 |
| CSO_KB_pH10 | 32.80 | 32.28 | 34.92 | 0.01 |
| CSO_CNT_pH12 | 29.14 | 21.92 | 48.91 | 0.04 |
| CSO_G_pH12 | 32.71 | 21,18 | 46.11 | - |
| CSO_KB_pH12 | 29.40 | 27.63 | 42.96 | - |

Table S3. ORR catalyst performance of each sample

| Sample | Onset Potential [V vs. RHE] | Current density at 0.464 V vs. RHE [mA/cm$^2$] | Electron transfer numbers at 0.464 V vs. RHE | Hydrogen peroxide yields [%] |
|---|---|---|---|---|
| CSO_pH10 | 0.766 | -3.47 | 3.67 | 16.54 |
| CSO_CNT_pH10 | 0.794 | -5.31 | 3.76 | 11.84 |
| CSO_G_pH10 | 0.807 | -4.49 | 3.47 | 26.51 |
| CSO_KB_pH10 | 0.843 | -5.58 | 3.17 | 41.64 |
| CSO_pH12 | 0.743 | -4.00 | 3.60 | 19.82 |
| CSO_CNT_pH12 | 0.834 | -5.56 | 3.71 | 14.47 |
| CSO_G_pH12 | 0.769 | -4.60 | 3.47 | 26.66 |
| CSO_KB_pH12 | 0.915 | -6.96 | 3.92 | 4.55 |
| CSO_CNT_pH12(co) | 0.728 | -1.71 | 2.43 | 80.41 |
| CSO_G_pH12(co) | 0.718 | -1.34 | 2.62 | 70.72 |
| CSO_KB_pH12(co) | 0.757 | -2.58 | 2.64 | 69.70 |
| 20 wt.% Pt/C | 0.960 | -5.57 | 3.71 | 14.40 |

Table S4. OER catalyst performance of each sample

| Sample | Onset Potential [V vs. RHE] | Potentials at reaching 10 mA/cm$^2$ [V vs. RHE] | Overpotentials at 10 mA/cm$^2$ [V vs. RHE] | Tafel Slope [mV/dec.] |
|---|---|---|---|---|
| CSO_pH10 | 1.526 | 1.625 | 0.395 | 83 |
| CSO_CNT_pH10 | 1.508 | 1.592 | 0.362 | 77 |
| CSO_G_pH10 | 1.491 | 1.601 | 0.381 | 101 |
| CSO_KB_pH10 | 1.341 | 1.575 | 0.345 | 126 |
| CSO_pH12 | 1.498 | 1.582 | 0.352 | 78 |
| CSO_CNT_pH12 | 1.446 | 1.580 | 0.350 | 110 |
| CSO_G_pH12 | 1.418 | 1.577 | 0.347 | 108 |
| CSO_KB_pH12 | 1.322 | 1.548 | 0.318 | 144 |
| CSO_CNT_pH12(co) | 1.546 | 1.733 | 0.503 | 168 |
| CSO_G_pH12(co) | 1.536 | 1.683 | 0.453 | 193 |
| CSO_KB_pH12(co) | 1.461 | 1.635 | 0.405 | 165 |
| $RuO_2$ | 1.470 | 1.659 | 0.429 | 162 |

Table S5. BET specific surface area measurement results for each sample

| Sample name | Specific surface area [$m^2/g$] |
|---|---|
| CSO_pH10 | 248.17 |
| CSO_CNT_pH10 | 229.56 |
| CSO_G_pH10 | 212.43 |
| CSO_KB_pH10 | 298.77 |
| CSO_pH12 | 146.20 |
| CSO_CNT_pH12 | 203.20 |
| CSO_G_pH12 | 208.62 |
| CSO_KB_pH12 | 169.88 |

## Calculation methods

Electrochemically active surface areas (ECSA) for each system were estimated from the catalytic surface's electrochemical double-layer capacitance ($C_{dl}$). CV method was used to measure the electrochemical $C_{dl}$. The potential was swept at different scan rates of 20, 50, 100, 200, 400, 600, 800, and 1000 mV $s^{-1}$, where no faradic current was observed. (Figure 7a and d). Then the $C_{dl}$ was estimated by plotting the $\Delta J = (J_a\text{-}J_c)$ at 1.27 V vs RHE as a function of the scan rate (Figure 7c).[1,2]

The $C_{dl}$ can be calculated using the following equation: $C_{dl} = d(\Delta j) / 2dV_b$

The ECSA can be calculated using $C_{dl}$, as follows: $ECSA = C_{dl} / C_s$

For the estimation of ECSA, a specific capacitance ($C_s$) value $C_s$ = 0.040 mF $cm^{-2}$ in 1 M KOH.[1,2]

## Notes and references

1. S.W. Chae, A. Shio, T. Kishida, K. Furutono, Y. Kojima, G. Panomsuwan, T. Ishizaki, Materials, 2024, **17**, 2963.

2. C. C. McCrory, S. Jung, J. C. Peters and T. F. Jaramillo, *J. Am. Chem. Soc.*, 2013, **135**, 16977-16987.

3. S. Karak, K. Koner, A. Karmakar, S. Mohata, Y. Nishiyama, N. T. Duong, N. Thomas, T. G. Ajithkumar, M. S. Hossain and S. Bandyopadhyay, *Adv. Mater.*, 2023, 2209919.